



## MINIREVIEW

View Article Online  
View Journal | View Issue

Cite this: *Nanoscale Adv.*, 2020, 2, 5152

## Therapeutic nanodendrites: current applications and prospects

Adewale O. Oladipo, \* Thabo T. I. Nkambule, Bhekile B. Mamba and Titus A. M. Msagati \*

Multidisciplinary efforts in the field of nanomedicine for cancer therapy to provide solutions to common limitations of traditional drug administration such as poor bioaccumulation, hydrophobicity, and nonspecific biodistribution and targeting have registered very promising progress thus far. Currently, a new class of metal nanostructures possessing a unique dendritic-shaped morphology has been designed for improved therapeutic efficiency. Branched metal nanoparticles or metal nanodendrites are credited to present promising characteristics for biomedical applications owing to their unique physicochemical, optical, and electronic properties. Nanodendrites can enhance the loading efficiency of bioactive molecules due to their three-dimensional (3D) high surface area and can selectively deliver their cargo to tumor cells using their stimuli-responsive properties. With the ability to accumulate sufficiently within cells, nanodendrites can overcome the detection and clearance by glycoproteins. Moreover, active targeting ligands such as antibodies and proteins can as well be attached to these therapeutic nanodendrites to enhance specific tumor targeting, thereby presenting a multifunctional nanoplatform with tunable strategies. This mini-review focuses on recent developments in the understanding of metallic nanodendrite synthesis, formation mechanism, and their therapeutic capabilities for next-generation cancer therapy. Finally, the challenges and future opportunities of these fascinating materials to facilitate extensive research endeavors towards the design and application were discussed.

Received 13th August 2020  
Accepted 3rd October 2020

DOI: 10.1039/d0na00672f

rsc.li/nanoscale-advances

## Introduction

Over the last few decades, conventional chemotherapies though effective have been found to be limited in terms of their treatment outcomes. This is because most chemotherapeutic drugs induce several deleterious effects due to their inability to distinguish between normal cells from cancerous cells. Moreover, the insufficient and/or poor accumulation of drugs at target sites and the menace of drug resistance in cancer treatment regimes continue to pose a great challenge.<sup>1</sup> These challenges have hampered the use of conventional chemotherapy, thus prompting the need for alternative novel strategies to improve treatment success.

The emergence of nanoparticle-based delivery systems as an ingenious approach to traditional therapies has been able to mitigate the problems commonly associated with chemo-drugs. The precise release and accumulation of drugs in specific cells, tissues, and organs have been the principal focus of nanoparticle-based treatment strategies. Nanoparticles can

improve the intracellular delivery of drugs to cancer cells while circumventing acute toxicity to normal cells either by active or passive targeting design. To reach their target, however, drug-laden nanoparticles must overcome a variety of highly complex cellular barriers.<sup>2</sup> Besides, nanoparticles can enter the cells *via* receptor-mediated endocytosis, a process whereby nanoparticles modified by targeting ligands with a specific affinity towards distinct receptors are enveloped by endosomes after entry into cells, leading to the generation of new membrane-enclosed vesicles.<sup>3</sup> These vesicles can bypass the clearance by phagocytes, thus leading to preferential accumulation of drugs at the target site.<sup>2,4</sup> Although nanoparticles have offered significant improvements as drug delivery systems, some concerns relating to their limited tissue penetration, poor systemic circulation, insufficient drug loading, instability, and toxicity still require considerable interventions for improved and efficient therapy.<sup>5–8</sup>

Among the metal nanoparticles with excess structural morphologies such as nanoplates, nanorods, nanocages, nanoprisms, nanostars, nanodumbbells, *etc.*,<sup>9,10</sup> nanodendrites are particularly unique and fascinating in their architectural design owing to their three-dimensional (3D) morphology with multiple dense arrays of branches of porous structure of the surface. The high density of defects on the surface may

*Institute for Nanotechnology and Water Sustainability (iNanoWS), College of Science, Engineering and Technology, University of South Africa, Science Park Florida, Johannesburg 1710, South Africa. E-mail: walexy20002001@gmail.com; msagatam@unisa.ac.za*



contribute to a significantly improved surface area to volume ratio when compared to smooth surface nanocrystals.<sup>11,12</sup> These defects can provide multiple binding sites on a single branch of a nanodendrite with numerous interconnected sub-branches,<sup>13</sup> thereby making it possible to achieve excellent features for multivariant applications such as catalysis,<sup>14</sup> drug delivery,<sup>15</sup> and hyperthermia cancer therapy.<sup>16</sup> As an example, nanodendrites have recently been reported to form various assemblies, including monometallic, bimetallic, and in a few cases trimetallic nanodendrites with superior tunable shape-dependent properties. These superior properties, especially those of noble metal-based systems, include high selectivity and sensitivity,<sup>17–19</sup> enhanced catalytic activity,<sup>20–22</sup> improved antimicrobial activity,<sup>23,24</sup> enhanced drug loading content,<sup>25,26</sup> and good stability and biocompatibility.<sup>27–29</sup> Moreover, the presence of multiple metals in the structure has provided possibilities for several morphological architectures and orientations of metallic nanodendrites, such as core-shell, alloy, mixed structures, and sub-clusters.<sup>30,31</sup> The promising physicochemically induced properties are due to the synergistic or multifunctional effect influenced by the combination of the two individual metals and have been widely investigated.

In spite of the problems related to the use of nanoparticle-based interventions in medicine, they still hold much potential in cancer therapy. A number of nanoformulations have been approved by regulatory agencies for use in cancer treatment.<sup>32,33</sup> These nanoparticle formulations exert minor side effects

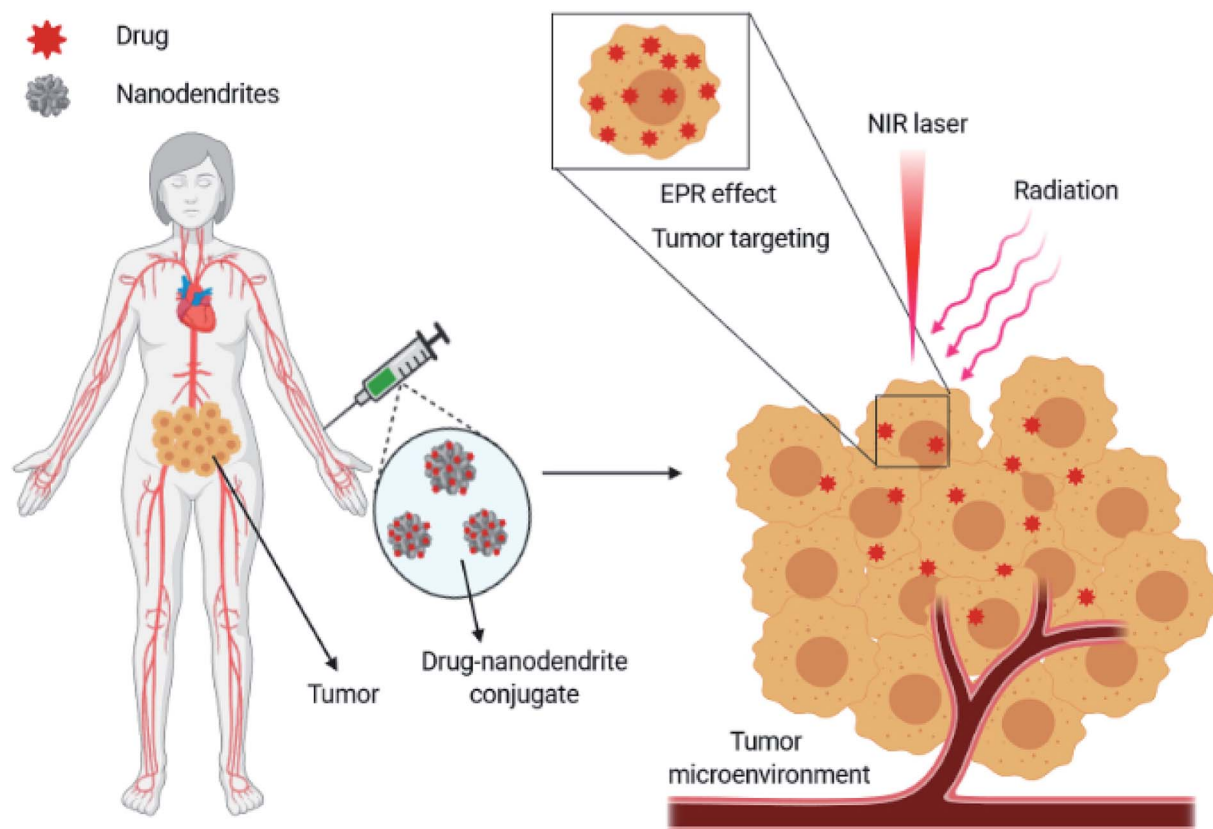
compared to conventional drugs. However, a focused review of metallic nanodendrites for promising therapeutic applications remains unavailable in the literature (Scheme 1). Consequently, in this minireview, we highlighted the types and properties of metallic nanodendrites considering their synthesis methods. Thereafter, recent progress in the development of dendritic-shaped nanoparticles with potential photothermal and stimuli-responsive therapeutic functionalities is discussed in detail. Eventually, we offer promising prospects in designing metallic nanodendrites for improved cancer therapy.

## Basis of metallic nanodendrites

This section highlights the basic concept of metallic nanodendrites: firstly, a discussion on the properties of metallic nanodendrites; secondly, an introduction to the types and methods of synthesizing metallic nanodendrites.

### Optical properties of metallic nanodendrites

Metallic nanodendrites (NDs) have been proven to have versatile potential applications in many fields and continue to attract research interest. Dendritic/branched structures with porous and uneven surfaces are known to provide an extremely large surface area with high-density active sites compared to smooth-surfaced nanocrystals. Complex morphologies such as nanodendrites can significantly maximize their photoabsorption



**Scheme 1** Applications of metallic nanodendrites as therapeutic agents in cancer therapy.



compared to nanorods, nanostars, and nanoshells. For example, Guo and co-workers reported that 3D Pt-on-Au bimetallic nanodendrites exhibited a broad extinction band which red-shifted to the NIR range resulting in a much higher electrocatalytic activity than core/shell Au@PtNPs with a rough surface.<sup>34</sup> The superior optical properties of the Pt-on-Au nanodendrites were attributed to the dipolar plasmonic oscillation dampening of the Au core by Pt deposition. The physical, chemical and electronic properties of metallic nanodendrites are immensely dependent on the spatial movement of the constituent electrons. When nanosized metallic particles (1–100 nm) interact with light illumination, free electrons positioned on the surface of the particles get excited, leading to an asymmetric distribution of the electron cloud over the nanoparticle. This electron displacement gives rise to a series of oscillations of the cloud of electrons on the surface, leading to a fascinating property termed as localized surface plasmon resonance (LSPR). Under an appropriate frequency of incident light, metallic dendritic nanostructures (e.g., gold, silver, palladium, platinum, copper) generate highly localized electrical fields within the confinement of the particle surface. Depending on the size, composition, dielectric properties, and structural orientation of the nanodendrites, the surface plasmon resonance can either be localized in the first near-infrared region (600–800 nm) or the second near-infrared region (900–1200 nm). These factors significantly influence the absorption and scattering properties of plasmonic metallic nanodendrites.

### Synthesis methods for metallic nanodendrites

Over the last few decades, a variety of research studies have been undertaken, which has led to several methods of synthesizing metallic nanodendrites being successfully developed. Diverse kinds of metallic NDs containing noble metals have been fabricated with many shapes or structural architectures. Currently, wet-chemical synthetic methods have been used as effective routes for the synthesis of metallic NDs.<sup>35</sup> The reduction of noble metal precursors based on their oxidation–reduction potential has made this route viable. Similarly, precise control over the size and morphology of metallic NDs using the dynamics of suitable stabilizers and coordination compounds to direct the nucleation process has been achieved with great success. Depending on their structural composition, metallic nanodendrites can be classified as either monometallic or bimetallic and in some cases, multimetallic in nature.

### Monometallic nanodendrites

Monometallic nanodendrites, as the name suggests, are nanoparticles of dendritic shape, consisting of only a single metal. The composition and shape of the metal atom determine the properties of these nanoparticles. Depending on the type of metal atoms present, for example, if they are metallic, transition, and magnetic nanoparticles, *etc.* monometallic nanodendrites are of different types. These nanodendrites can be prepared using different methods; however, the most widely used method is the wet chemical method. Control over the morphology of metal nanodendrites is critical in

nanomedicine, as it is in many fields such as catalysis, optics, and biomedicine. The structural morphology of metallic nanodendrites can be tailored to enhance their activity and ultimately performance. Several modalities have been proposed as a strategy to uniquely tailor and manipulate the reaction kinetics and activity of metal nanodendrites. One such way is the use of a gas atmosphere like CO, H<sub>2</sub>, NH<sub>3</sub>, *etc.*, which can serve as a surface confining agent for assisting the morphology control.<sup>36,37</sup> Gas atmospheric environments are believed to not only lower the reduction temperature but equally remove weak coordinating ligands, therefore, regulating the formation mechanism. This templateless and seedless method enables specific adsorption onto certain facets of porous structures of Pt using different gases.

Another method for tailoring the dendritic-structure of metallic nanoparticles is the seed-mediated method. A lot of fascinating studies that highlighted the synthesis of Au, Pd, Pt, *etc.* monometallic nanoparticles with distinctive branches on their surface have been reported.<sup>38–40</sup> The formation of metal nanodendrites has been reported to be largely dependent on the shape-directing agent used during the growth process<sup>41,42</sup> (Fig. 1). In many reports, the branches of dendritic-shaped nanoparticles are relatively large and random. To overcome this challenge, Pd nanodendrites with uniform perpendicularly ordered channels synthesized using hexadecylpyridinium chloride (HDPC) at ambient temperature have been recommended as a sustainable solution.<sup>38</sup> With no pre-formed seed required as a template, the HDPC acting as a shape-directing agent was found to be a critical element in controlling the final architecture because of the formation of a higher degree of surface atoms during the growth process. This process led to the formation of porous nanodendrites with perpendicular pore channels in a single reaction step.

Pd nanodendrites have also been obtained by adding a Pd precursor to octadecylamine (ODA), acting as both the surfactant and solvent, under a strong reducing agent (ascorbic acid) at high temperature.<sup>39</sup> The Pd nanodendrites prepared using this approach involved both the ODA and ascorbic acid at a higher temperature. The reduction of the Pd precursor under these conditions allowed for controlling the growth kinetics of the nanocrystals and ultimately the morphology of the products. Moreover, the final Pd nanodendrites were distinct with a three-dimensional architecture and monodisperse.

Interestingly, the multifunctionalities of nanodendrites can also be tailored by adjusting some synthetic parameters during the formation.<sup>43</sup> Recently, Qui *et al.* reported the influence of long-chain primary amines (butylamine, dodecylamine, octylamine, hydroxylamine, octadecylamine, and oleylamine) and solvents (ethanol and chloroform) on the dendritic-morphology and degree of branching of gold nanodendrites. In this strategy, primary amines of different carbon chain lengths were employed as structure directing agents in a seed-mediated reduction protocol with ascorbic acid as the reductant. Several factors, including the type of primary amines, type of solvent, concentrations of amines, amount of seed volume, type of gold seed shape, *etc.*, all play a crucial role in influencing the degree of branching, morphology, and size evolution of the Au





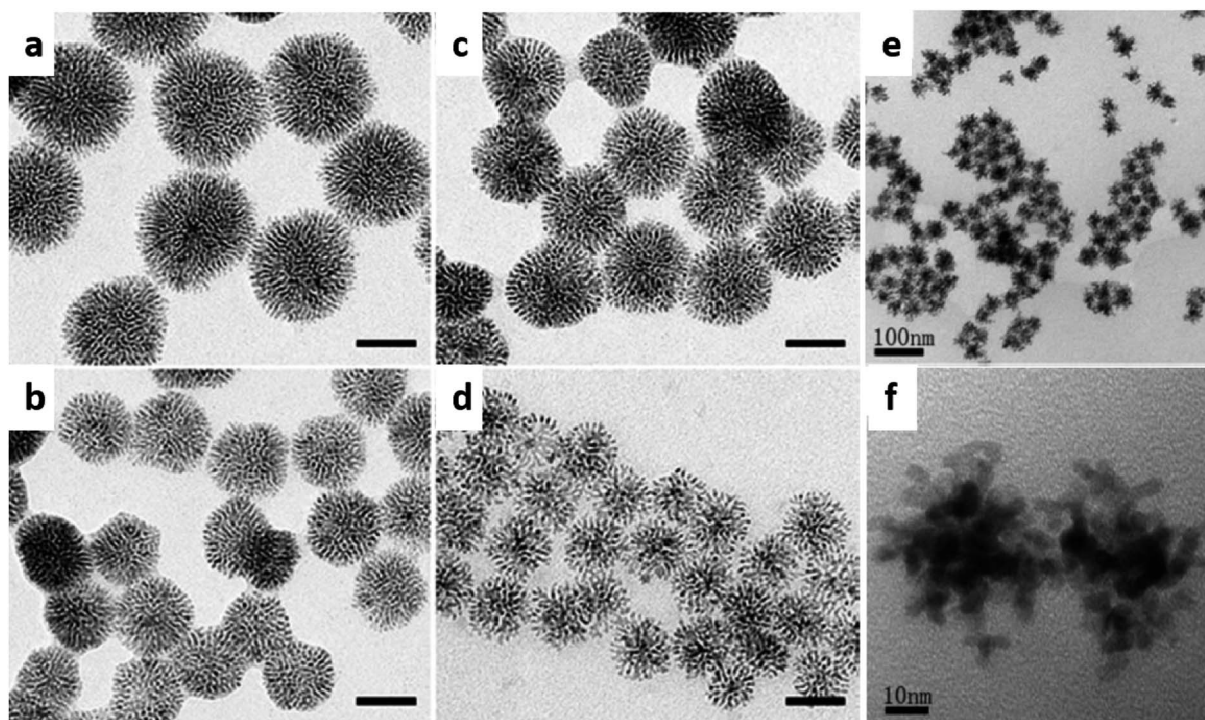


**Fig. 1** TEM images of Pd nanodendrites synthesized using hexadecylpyridinium chloride (HDPC) surfactant at (a) 20 °C, (b) 400  $\mu$ L ascorbic acid, (c) 300  $\mu$ L ascorbic acid, and (d) 50 °C under similar conditions. Adapted with permission from ref. 38 Copyright 2013 Wiley-VCH. TEM image of Pd nanodendrites synthesized using octadecylamine (ODA) surfactant at (e) low resolution and (f) high resolution. Adapted with permission from ref. 39 Copyright 2014 Royal Society of Chemistry.

nanodendrites. Specifically, the degree of branching was found to greatly impact the plasmonic properties of the nanodendrites.<sup>40</sup>

Another strategy, the laser irradiation method, has been used for fabricating and controlling the sizes and surface architectures of various types of nanoparticles, including metallic nanodendrites. The utilization of light amplification through stimulated emission of radiation provides an energy source for irradiating solid materials.<sup>44</sup> During this process, tremendously high energy is focused on a solid at a specific point to generate surface atoms in the light-absorbing material.<sup>45</sup> The fabrication of bimetallic nanodendrites with multifunctional systems using laser light as a versatile tool has generated some interest. Intense and multi-branched Ag@Au bimetallic nanodendrites with optically tunable surface plasmon resonance were achieved *via* a laser-driven photochemical route.<sup>46</sup> With continuous laser irradiation of a well-polished Au metal dipped into an Ag liquid solution at a wavelength of 532 nm, a slow and moderate nucleation growth mechanism allowed for controlled manipulation of the dendritic-shaped nanoparticles, thereby resulting in high-purity nanostructures.

### Bimetallic nanodendrites

Bimetallic nanodendrites have attracted immense attention in recent years. This is attributed to the nanocrystals composed of two individual metals, either forming a homogenous alloy or a heterogeneous mixture with distinct properties when

compared to monometallic nanodendrites.<sup>47</sup> Typically, the fabrication of bimetallic nanodendrites is more complicated than monometallic nanodendrites. While many studies with sufficient understanding of the growth mechanism have been reported for the shape-selective growth of monometallic nanodendrites, the same rules simply do not apply to bimetallic nanodendrites. The introduction of a second metal in the synthesis could have a significant effect on the nucleation and growth processes of nanodendrites. To date, many fabrication methods have been developed for bimetallic nanodendrites. Among the synthetic methods developed are co-reduction, template, and galvanic replacement methods.

As for the chemical co-reduction method, it generally involves the use of two individual metal (active and support) precursors under a suitable reducing agent(s) that can reduce the metal ions to their atoms in a single step.<sup>48</sup> The incorporation of surfactants into the reaction enables the capping of both nanocrystal surfaces intending to direct the shape and size. The formation of the dendritic-shaped bimetallic nanoparticles is significantly dependent on the reduction rate and ionic interaction of the two metals involved. The formation mechanism of the dendritic AuPt bimetallic system with ascorbic acid as the reducing agent was recently highlighted by He and co-workers.<sup>18</sup> In this reaction, AuPt nanodendrites with a porous and tunable composition were synthesized by changing the molar ratio of  $\text{Au}^{3+}/\text{Pt}^{2+}$  precursor ions. With a well-defined intermediate lattice plane, the structural orientation indicated an attachment mechanism for the formation of AuPt nanodendrites from



smaller nanodots. During the formation of bimetallic nanodendrites, the different reduction rates of the metal ions often lead to the generation and nucleation of one metal as seeds first before the deposition of the second metal.<sup>49</sup> This process often results in a large lattice mismatch and high bond dissociation energies between the two metals, which favor dendritic-island growth mode formation.<sup>50</sup> This method provides the advantage of preparing homogenous bimetallic nanodendrites with a high loading of metals (>70 wt%). By manipulating the reaction kinetics, several bimetallic nanodendrites with different metal combinations have been achieved.

Another important synthetic strategy for bimetallic nanodendrite formation is the template-controlled method. This approach enables the synthesis of bimetallic nanodendrites more easily than the co-reduction method because the nanocrystals of one pre-formed metal can be used as a template to direct the growth of the second metal.<sup>51,52</sup> The relative reduction potential between the seed template and metal ions provides the driving force that allows for the deposition of newly reduced metal atoms over the solid nanocrystal-template support (Fig. 2). This route provides the possibility for precise control of the composition and morphology of the final nanoparticles by changing the molar ratio of the reactants as well as the shape of the sacrificial template nanocrystals, which in most cases are of different morphologies.<sup>53–56</sup> This synthetic strategy leads to the formation of bimetallic nanostructures with a porous and high surface area within a short reaction time.<sup>51,57</sup>

Over the past years, the template method has been used for synthesizing bimetallic nanodendrites based on gold (Au), silver (Ag), platinum (Pt), and palladium (Pd) with tunable properties. Due to the several advantages provided by the

template method, many researchers have extended the physicochemical opportunities for control offered by this method. Recently, gold core-palladium nanodendrites (Au@PdNDs) were synthesized *via* a one-pot route by Zhou and co-workers.<sup>39</sup> In this reaction, a pre-formed gold seed was used as the sacrificial template to direct the growth of palladium dendrites on the gold seed. The effects of the reaction conditions (high temperature, 160 °C; capping agent and solvents, octadecylamine (ODA); and reducing agent, ascorbic acid) were critical to the formation of the bimetallic nanodendrites. The newly reduced Pd atoms attached to the heterogeneous Au seeds *via* a rapid growth mechanism, thereby leading to Au@PdNDs formation. As mentioned, the geometry of the template seed is important in dendritic-shape formation.

As a modified template method incorporating a seed-mediated deposition reaction, Tan and co-workers reported surfactant-free Au@Pt dendritic-shaped nanoparticles using a modified template method.<sup>22</sup> Pt precursor solutions of different volumes were added to pre-formed spiny-shaped AuNPs with ascorbic acid as a reductant at 90 °C. The spiny AuNPs provided a nucleation focal point for the reduced Pt atoms to uniformly grow and decorate the spiny AuNP surface. This reaction mechanism is possible when a strong reducing agent is used and the reduction potential of the second metal (Pt) is more negative compared to the sacrificial template metal (Fig. 3). Moreover, the geometry of bimetallic nanodendrites synthesized *via* the template method (Fig. 4) has also been reported to be largely dependent on the metal-metal bond strength, concentration, and rate of deposition of precursors, and coating thickness of the sacrificial template.<sup>51,59,60</sup>

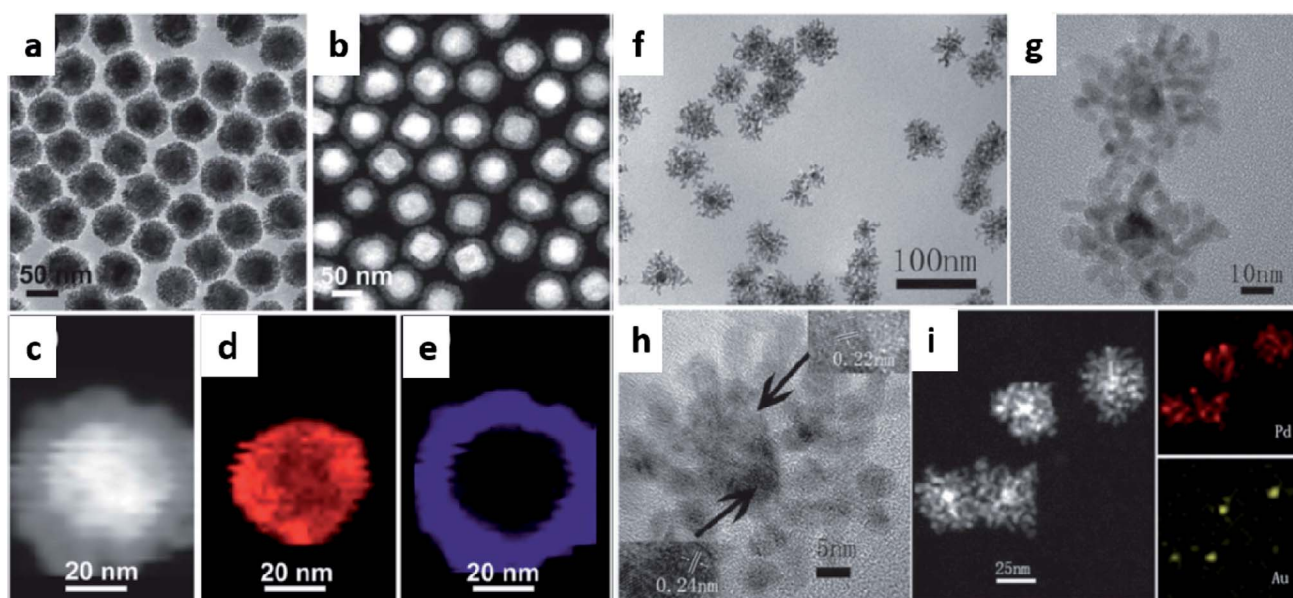


Fig. 2 (a) TEM image, (b and c) HAADF-STEM images, (d and e) EDX elemental mapping of Au and Pd, respectively of Au@Pd core-shell nanodendrites synthesized from Au polyhedral seeds as a template. Adapted with permission from ref. 58 Copyright 2013 Royal Society of Chemistry. (f) TEM image, (g and h) HRTEM images, (i) HAADF-STEM image and EDS elemental mapping of Pd and Au, respectively of Au@Pd core-shell nanodendrites synthesized from Au spherical seeds as a template. Adapted with permission from ref. 39 Copyright 2013 Royal Society of Chemistry.





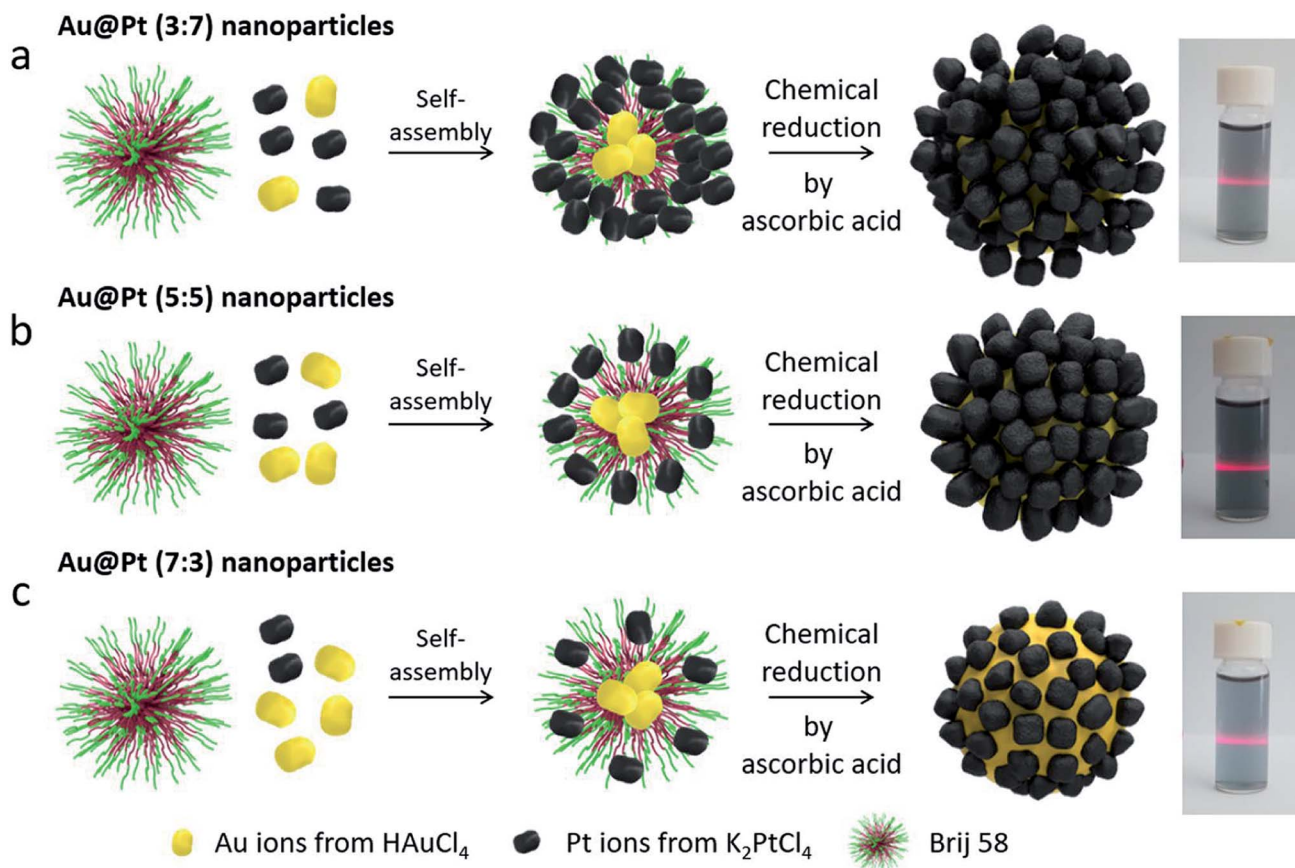


Fig. 3 A graphical explanation of Au@Pt nanoparticles under three different stoichiometries (a) 3 : 7, (b) 5 : 5, and (c) 7 : 3 (left), and photographs of the Tyndall effect on the nanoparticle suspensions in solution (right). Adapted with permission from ref. 61 Copyright 2019 Springer Nature.

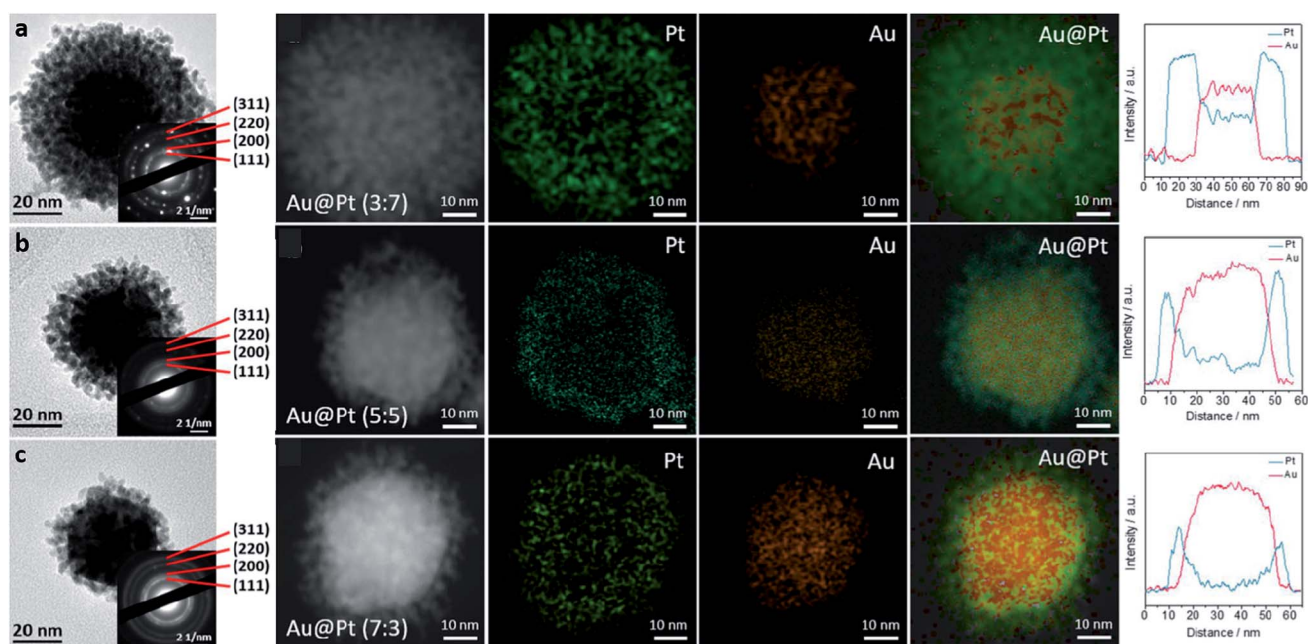


Fig. 4 (a–c) TEM images of Au@Pt nanodendrites at three different Au : Pt ratios (a) 3 : 7; (b) 5 : 5, and (c) 7 : 3. Insets showing the corresponding SAED patterns and HAADF-STEM images with corresponding Au and Pt elemental mappings, and line scans. Adapted with permission from ref. 61 Copyright 2019 Springer Nature.



## Therapeutic applications of metallic nanodendrites

As a distinct nanostructure, metallic nanodendrites possess a three-dimensional (3D) large surface area that can be adjusted. This section discusses several applications of metallic nanodendrites with emerging therapeutic functionalities including photothermal, radiotherapy, theranostics, and drug delivery applications (Table 1).

### Metallic nanodendrites for photothermal applications

A non-invasive treatment strategy that offers increased tumor permeability, enhanced tumor uptake of biomaterials, and selective destruction of tumor cells is photothermal therapy (PTT). This emerging cancer therapy utilizes the heat generated locally under light interaction with a light-absorbing nanomaterial to kill cancer cells.<sup>62</sup> Therefore, the extravasation of the photothermal agent into the tumor region significantly increases. For a maximal hyperthermia response of the nanomaterials, absorption under near-infrared (NIR) laser light (700–1300 nm) is very essential. Over the years, a myriad of nanostructures including graphene oxides,<sup>63</sup> metal nanoparticles,<sup>64,65</sup> black phosphorus,<sup>66</sup> carbon nanotubes,<sup>67</sup> metal-organic frameworks (MOFs), *etc.*<sup>68</sup> has been proposed as candidates for photothermal therapy. When plasmonic nanostructures change shape from spheres to other morphological architectures (shells, cages, and dendrites), the optical absorption can be maximized in the NIR region. Similarly, the change in shape also results in a large surface area and can be controlled for optimal absorption.

Interestingly, metallic nanoparticles are preferred as hyperthermia materials due to their biocompatibility, tunable surface plasmon resonance (SPR) absorption, and ease of surface modification. Metallic nanoparticles of Au, Ag, Pd, Ru, Cu, and Pt origin have been intensively researched and deployed as ideal photothermal agents.<sup>69–73</sup> To improve the ability of metallic nanostructures for this purpose, their morphology needs to be controlled, thereby enhancing the therapeutic efficiency. Considering their structural orientation, Qiu and co-workers proposed that gold nanodendrites could be used as photothermal agents.<sup>74</sup> By tuning the degree of branching of the nanodendrites, the optical properties were also tuned in the

NIR region, thereby leading to a significant performance in the photothermal response (Fig. 5). Gold nanodendrites with a higher degree of branching were found to be more efficient photoabsorbers under lower wavelength laser irradiation, while nanodendrites with a lower degree of branching were discovered to destroy tumors under higher wavelength laser irradiation. The resulting wavelength-dependent photothermal effects highlighted the importance of the dendritic degree of branching and allowed for the appropriate laser wavelength required for tailored cancer therapeutic performance.

In many plasmonic photothermal nanostructures, NIR light is predominantly used; hence, it is important to appropriately select nanostructures that exhibit higher NIR light absorption.<sup>75</sup> Particularly, in biomedical applications, NIR laser light (800–1100 nm) has been extensively used because it can induce deep penetration into the body owing to the scattering of photons by biological tissues (water, blood, and fat) and reduced absorption.<sup>76</sup> Various materials of bimetallic nanodendrites comprising gold, platinum, and palladium have been broadly studied for their photothermal effects. Their longitudinal surface plasmon resonance (LSPR) can be tuned to the NIR range and in most cases, the synergistic effects can be effectively harnessed compared to their monometallic counterparts. With the rapid development of photothermal agents, various structural architectures have evolved with the aim of tuning the LSPR to NIR range. For example, novel gold nanoshells with multiple branches (BGSs) possessing ultrastrong NIR absorption were synthesized using a dual-template method in which silver nanocrystals (AgNCs) were used as a sacrificial template.<sup>77</sup> The anisotropic growth process of the BGS synthesis enabled a controlled tunability of the length, diameter, and density of the branches. Moreover, *in vitro* and *in vivo* experimental results showed that the BGSs exhibited an intense NIR photothermal heat conversion which selectively kills cancer cells upon irradiation with a laser. Recently, McGrath *et al.* designed bimetallic nanodendrites (Pd–Au) in which multiple gold nanoparticles were deposited over branched palladium seeds *via* a seed-mediated method for photothermal therapy.<sup>78</sup> Under NIR laser irradiation at 808 nm, Pd–Au bimetallic nanodendrites caused the complete destruction of HeLa tumor xenografts in a mouse model (Fig. 6). The enhanced

**Table 1** A summary of the various metallic nanodendrites and their therapeutic applications

Metallic NDs	Composition	Applications	Ref.
AuNDs	Gold	Imaging and photothermal therapy	74
AuNDs	Gold	Photothermal and chemotherapy	90
PtNDs	Platinum	Radiotherapy	85
AuNDs	Gold	Imaging and photothermal therapy	77
PdAuNDs	Gold-over branched palladium	Photothermal therapy	78
Au@PtNDs	Gold-core platinum shell	Imaging and photothermal therapy	79
Au@PtNDs	Gold-core platinum shell	Imaging, photothermal, and radiotherapy	81
PtRuNDs	Alloyed platinum–ruthenium	Imaging, photothermal, and radiotherapy	86
Au@PdNDs	Gold-core palladium shell	Stimuli-responsive drug delivery	15
Au@PtNDs	Gold-core platinum shell	Imaging, photothermal, and chemotherapy	89





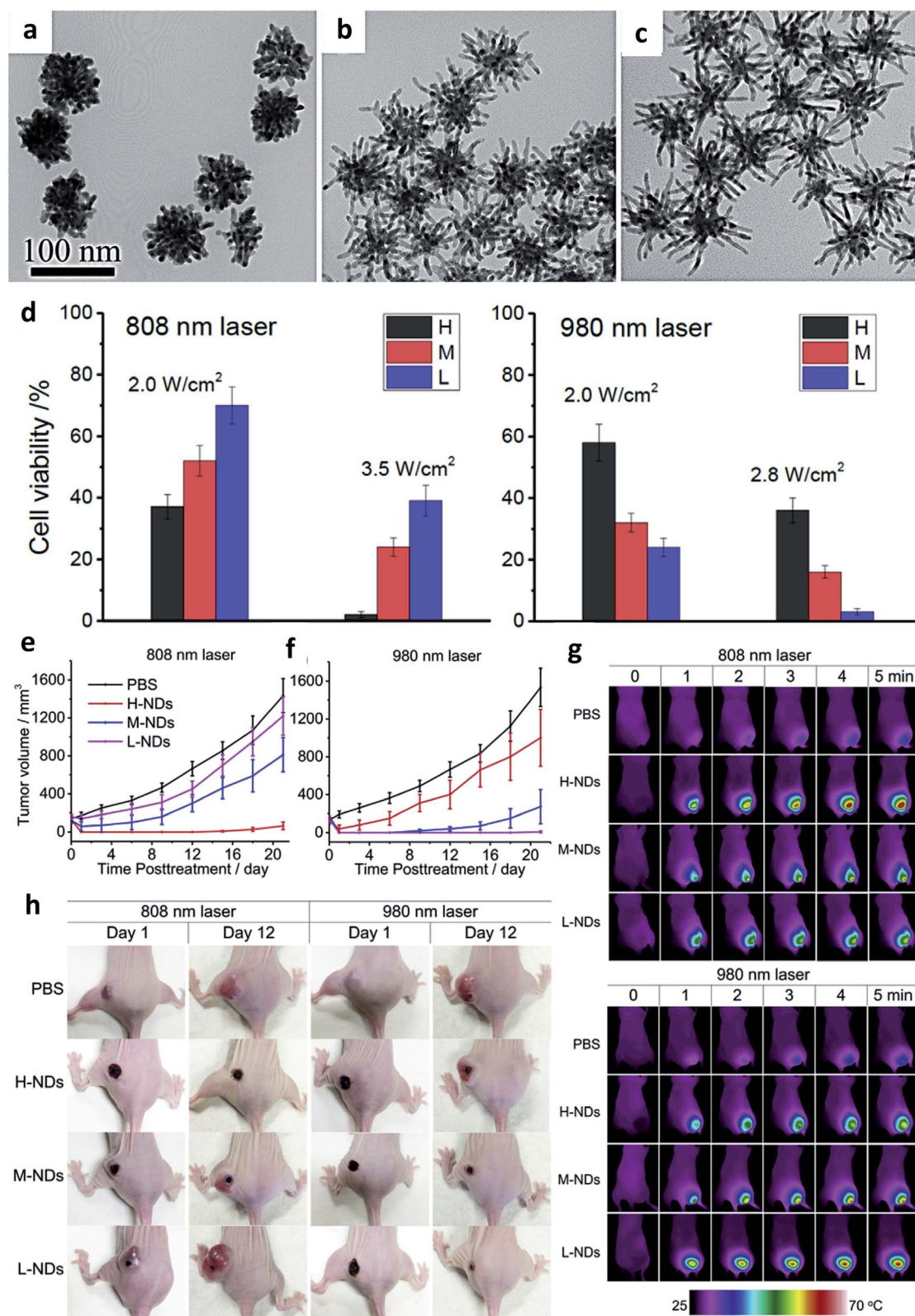


**Fig. 5** TEM images of synthesized gold nanodendrites of (a) high, (b) medium, and (c) low degree of branching, (d) cell viability study of high, medium and low gold nanodendrites after irradiation at 808 nm and 980 nm laser power densities, (e and f) tumor volume changes after photothermal treatment of MCF-7 tumor xenografts of different gold nanodendrites of varying degree of branching, (g) real-time infrared imaging of temperature changes inside tumors during photothermal ablation, and (h) photographs of a representative mouse in each group on day 1 and day 12 after photothermal treatment. Adapted with permission from ref. 74 Copyright 2016, Elsevier.





photothermal hyperthermia was attributed to the electronic coupling and interaction between the gold and palladium, which red-shifted the maximum absorption of gold nanoparticles to the NIR region. The importance of high light-to-heat conversion performance resulting from strong absorption in the NIR region cannot be overemphasized in the fabrication of an excellent photothermal agent. To this effect, Yang *et al.* fabricated dendritic-structured bimetallic Au@Pt nanoparticles using a one-step ultrasound-mediated method.<sup>79</sup> To prevent protein adsorption and subsequent clearance by phagocytes, the dendritic nanoparticles were coated with methoxy-PEG-thiol molecules. The SPR coupling of the Au core and Pt dendritic shell effectively

enhanced the absorption properties of the Au@Pt nanoparticles, thereby culminating in a high photothermal conversion efficiency of 44.4% under an 808 nm laser when compared with monometallic AuNPs. *In vivo* experiments demonstrated the dose-dependent cellular anti-proliferation capacity of the Au@PtNPs with enhanced NIR absorption for photothermal application in a tumor mouse model.

### Metallic nanodendrites for radiotherapy applications

The minimal invasiveness of photothermal therapy has also allowed for combination therapy in clinical cancer therapy. One

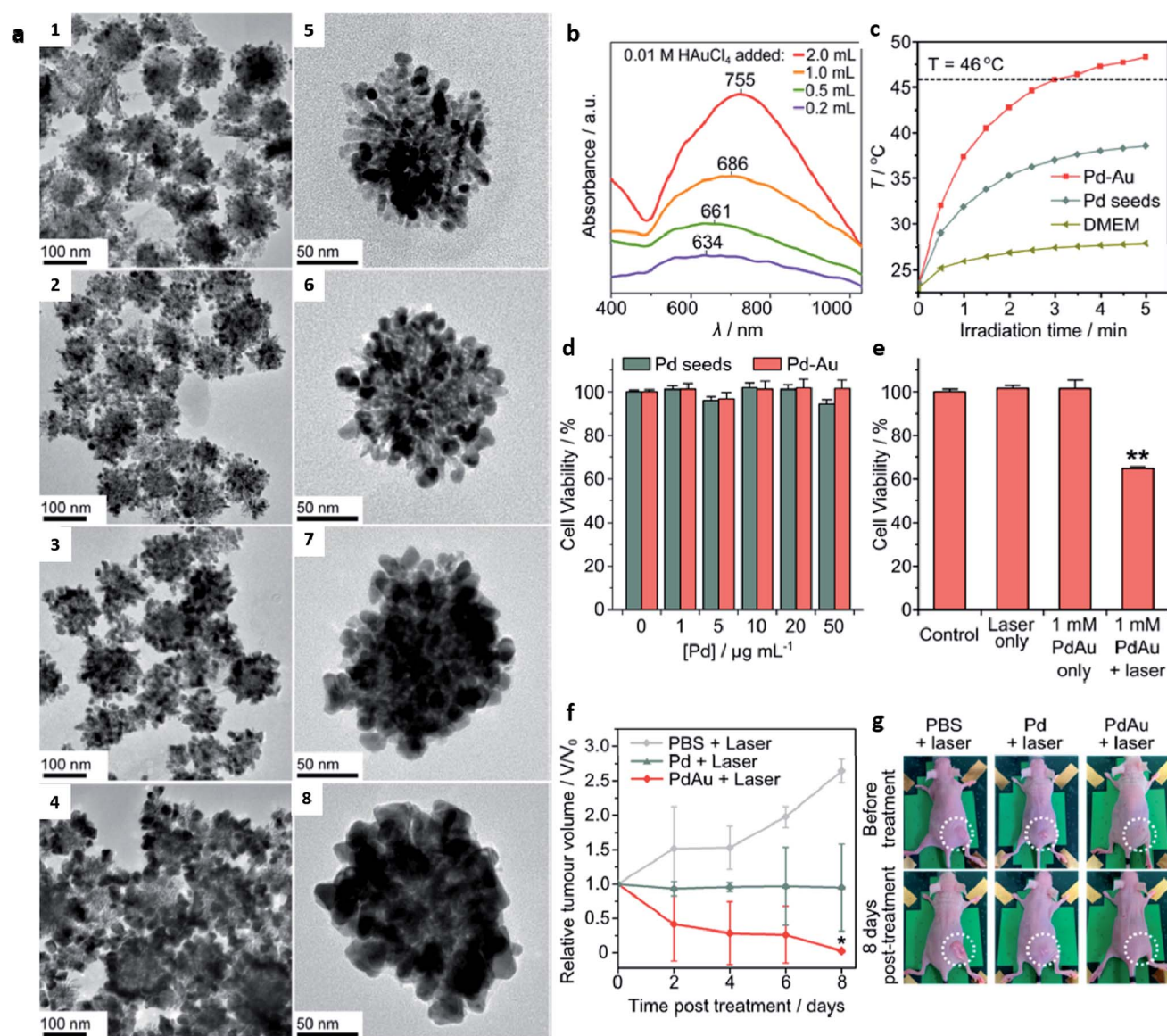


**Fig. 6** (a1–4) Lower and (a5–8) higher magnification TEM images of synthesized Pd–Au nanodendrites, (b) absorption spectra of Pd–Au nanodendrites synthesized with different volumes of 0.01 M Au<sup>3+</sup>, (c) temperature changes of Pd seeds and Pd–Au nanodendrites under laser irradiation at the same concentration of 50 μg mL<sup>-1</sup>, (d) MTT cell viability assays of Pd seeds and Pd–Au nanodendrites incubated in HeLa cells at varying concentrations, (e) cell viability assay behavior of Pd–Au nanodendrites incubated in HeLa cells under laser irradiation, (f) tumor volume changes in HeLa cell xenografts after photothermal treatment (808 nm, 3 W cm<sup>-2</sup>) of PBS, Pd seeds, and Pd–Au nanodendrites at 50 μg mL<sup>-1</sup> Pd concentration, and (g) representative photographs of mice before and after laser irradiation treatment of tumor sites for 30 min at 3 W cm<sup>-2</sup> on day 8 in each group. Adapted with permission from ref. 78 Copyright 2015 American Chemical Society.



such treatment strategy used in combination with PTT is radiation therapy (RT). Radiation therapy employs highly ionizing radiation generated from charged particles ( $\alpha$ ,  $\beta$ -particles), X-rays, gamma rays, and neutrons to induce serious damage to cancer cells/tumor mass shrinkage *via* DNA base pair breakage.<sup>80</sup> This powerful combination of strategies has facilitated therapeutic efficiency due to the significance of their merits and the avoidance of their demerits. As a demonstration of the feasibility of this combination technique, Liu and co-workers designed PEGylated Au@Pt nanodendrites for synergistic PTT/RT integrated into a single platform.<sup>81</sup> The broad absorption of the Au@PtNDs stretched beyond the first NIR window due to the growth of the Pt branches, thereby enhancing the PTT conversion efficiency. Moreover, the high *Z* number of both Au and Pt afforded a lethal radiation dose induction; thus, the combinatory effect of PTT and RT resulted in enhanced tumor growth suppression accompanied by a significant computer tomography (CT) imaging signal.

Similarly, nanoparticles synthesized from high atomic number (*Z*)-based elements such as Au, Ag, Pt, Gd, Fe, I, *etc.*<sup>82–84</sup> have the potential to improve the efficiency of radiotherapy. This has been attributed to their ability to allow more absorption of radiation per unit mass in tumors thus enhancing the radiation dose.<sup>83</sup> As reported by Muhammad *et al.*, platinum nanodendrites (PtNDs) of different sizes were synthesized using a chemical reduction method and deployed as radiosensitizers in photon beam radiation therapy.<sup>85</sup> The PtNDs of all sizes exhibited a two-fold radiosensitization enhancement upon 6 MV photon beam irradiation towards HeLa cells. More significantly, the sensitization enhancement ratio (SER) was found to be dependent on the size of PtNDs, thereby demonstrating the potential of PtNDs in radiotherapy. Besides, the need for improved cancer therapy efficiency has led to the development of nanostructures with metal combinations of emerging materials of choice in nanomedicine. By combining the intrinsic properties of upcoming and promising therapeutic metals like ruthenium, rhodium, *etc.* with already established metals like gold, silver, platinum, *etc.* new types of metallic nanodendrites such as platinum–ruthenium (PtRu) nanodendrites have continued to evolve.<sup>86</sup> Functionalized with a multifoliate receptor that can overcome clearance by glycoproteins and improve targeting ability, the uniquely fabricated PtRu bimetallic nanocomplexes demonstrated a combined photothermal/radiation therapy in a synergistic manner as well as computer tomography (CT) imaging capabilities. This has led to significant advances in the multifunctional dimensions concerning the simultaneous treatment and multimodal image-guided nanoplatforms. In addition, the combination of treatment approaches has been able to address the limitations of a single treatment protocol with great success.

### Metallic nanodendrites for stimuli-responsive drug delivery applications

The use of stimuli-responsive or smart nanostructures as nanocarriers for drug delivery is essential to improve therapeutic efficiency while reducing undesired side effects. These

intelligent nanocarriers have been engineered to experience activated responses when exposed to modifications in the environment. Recently, metallic nanodendrites have been increasingly used as drug delivery nanocarriers due to their tunable plasmonic properties, localized heat generation, and large surface area. These properties help to remotely release their payloads under stimuli-triggered conditions. The stimuli could be internal (pH, enzymes, antigens, *etc.*), which are related mostly to the cellular/tissue status or external (light, heat, magnetic field, ultrasound, *etc.*), which require an externally controlled applied stimuli response in nature.<sup>15,75</sup> These special effects have been widely used to initiate drug release at any specific site and have also been used to accumulate drugs at the selected target before their release. The resultant effect of this delivery system is the minimization of poor accumulation and biodistribution of drugs hence, mitigating undesirable side effects and enhancing therapeutic efficacy.

Recently, our group designed bimetallic gold-core palladium nanodendrites (Au@PdNDs) that were conjugated with the anticancer drug doxorubicin (DOX) with potential drug delivery applications.<sup>15</sup> Since specific substrates respond to changes in local pH, nanocarriers can be designed and exploited for modulating drug release. We used negatively charged nanodendrites to electrostatically load positively charged DOX molecules in a heterogeneous binding mechanism. The dendritic-shaped bimetallic nanostructured-incorporated DOX demonstrated improved stimuli-responsive properties under a typical cellular microenvironment (pH, temperature, enzymes). pH-Responsive drug nanocarriers are stable under physiological conditions ( $\sim 7.4$ ), but under acidic microtumor environments, they release their payload. This fascinating property has been attributed to the spatial heterogeneous blood flow within tumor vessel interstitial fluidics, resulting in a compromised metabolic environment, which decreases the pH to below 6.5.<sup>87</sup> The use of doxorubicin in the treatment of diverse cancers has been confirmed to induce reactive oxygen species (ROS) and oxidative damage in most major organs.<sup>88</sup> To mitigate this injury, Yang *et al.* proposed porous Au@Pt nanoparticles with dendritic architecture as a therapeutic platform for combined chemo–photothermal tumor therapy.<sup>89</sup> Hybrid nanodendritic composites have been designed to combine the hyperthermia plasmonic properties with thermoresponsive properties of conjugates for controlled drug delivery. The porous nature of the Pt dendritic shell of the Au@Pt bimetallic nanoparticles afforded a 3D capacity for DOX loading and reduced oxidative stress associated with drug induction (Fig. 7). The DOX-loaded Au@Pt nanoparticles were modified with cRGD, a tumor-targeting peptide that can evade detection by phagocytes and specifically binds to overexpressed integrin receptors on the surface of tumors. The peptide coating also enhanced the nanodendrite biocompatibility thereby improving its tumor accumulation and biostability. The Au@Pt nanoparticles displayed strong and intense absorption in the NIR region, which triggered the release of the drug *via* heat and light under 808 nm laser irradiation. This combination method significantly suppressed the growth of breast cancer and impacted the antioxidative effect on oxidative stress damage *in*



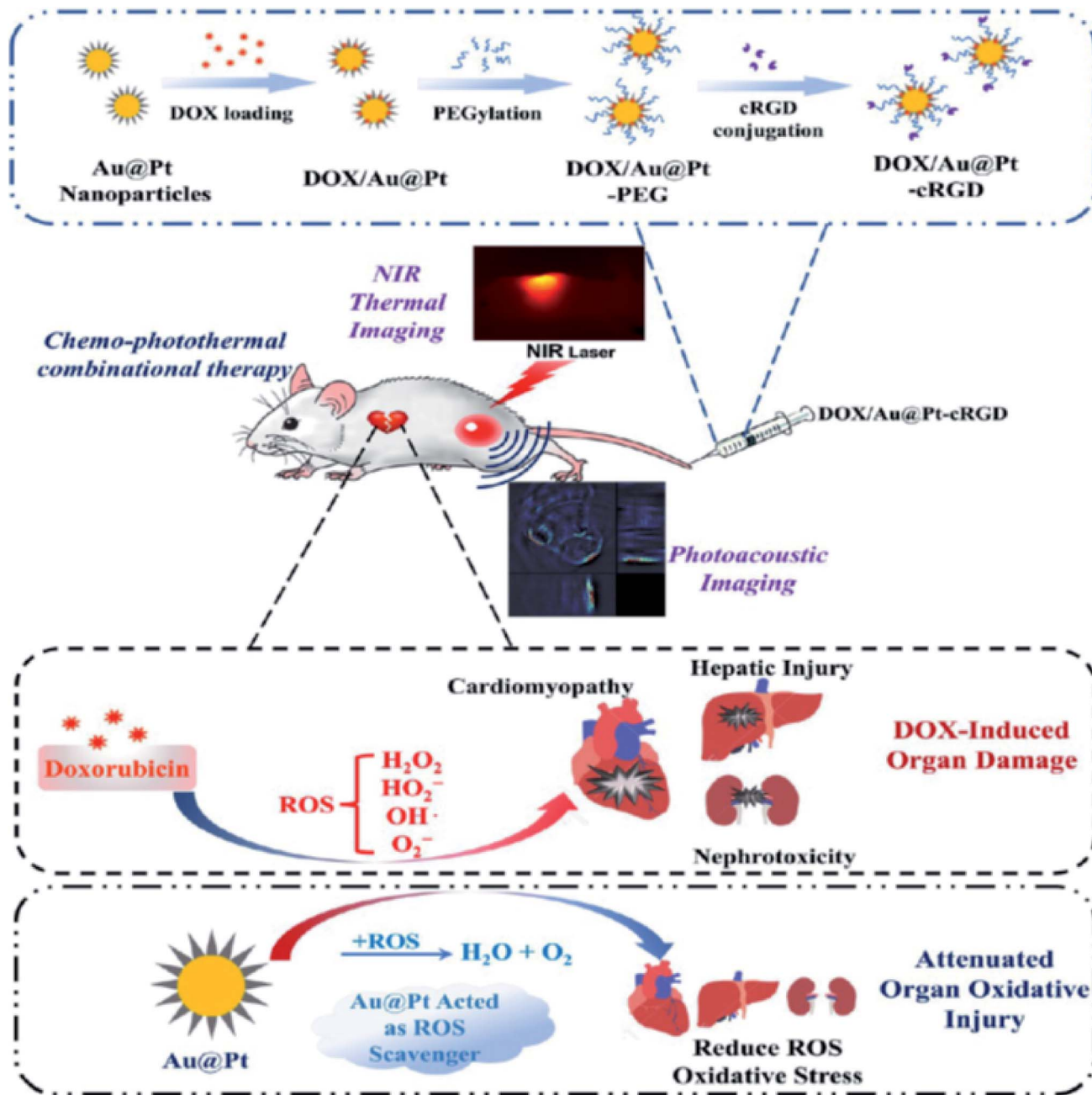


Fig. 7 Schematic illustration of the construction of DOX-loaded Au@Pt-cRGD, and ROS scavenging activity of the Pt shell of the bimetallic Au@Pt nanodendrites during chemo-photothermal therapy. Adapted with permission from ref. 89 Copyright 2018 American Chemical Society.

*in vivo* in an MDA-MB 231 tumor-bearing mouse model. This technique not only resulted in light-induced hyperthermia with an eventual tumor permeability, but also resulted in triggered drug release precisely to the targeted site. Although nanodendrite-based drug delivery for cancer treatment has demonstrated fascinating therapeutic efficiency, researchers have continued to further interest in the synergistic approach by combining two or more treatment strategies. This has resulted in the achievement of a significant improvement in anticancer efficacy. More recently, a multifunctional drug delivery system with synergistic chemo-photothermal therapy was reported by

Liu and co-workers.<sup>90</sup> To achieve this, gold nanobranched particles coated with a natural compound, betulinic acid (BA), encapsulated into liposomes that exhibited broad NIR absorption under laser irradiation were fabricated *via* a simple and surfactant-free protocol. The drug BA is a naturally occurring plant-derived pentacyclic triterpenoid with proven anticancer potential. Under NIR laser irradiation of  $1.5 \text{ W cm}^{-2}$  for 2 min, a rapid conversion of light to heat led to the controlled release of the BA, mediated by the high photothermal conversion efficiency of the gold dendritic nanoconjugate. The improved cellular uptake of the nanocarrier resulted in sufficient





intracellular accumulation with outstanding tumor growth suppression (87%), much higher than photothermal therapy or chemotherapy alone, therefore, suggesting the synergistic antitumor effect of the nanocarrier.

## Conclusion and future opportunities

This mini-review focused on the current advances in the deployment of dendritic-shaped metallic nanostructured systems, including several strategies that enable control over the morphological evolution as well as features that are pivotal in the activities of their structure–performance interactions. As we have highlighted, the main driving force for dendritic shape-directed formation is the surfactant. Besides, the chemical composition, shape, and size of nanodendrites are fundamental features for property-induced functional applications in biomedicine. Due to their diverse unique characteristics, the fascinating advantages of the multifunctional capabilities of nanodendrites can be evaluated for their development for more sophisticated and practical applications. For instance, aside from photothermal, radiotherapy, and drug delivery applications, one can design metallic nanodendrites as potential photosensitizers for use in photodynamic therapy either alone or in combination with other treatment methods. Moreover, the high absorption cross-section of metallic nanodendrites may potentially be utilized in photoacoustic imaging of cells in a 3D-culture system in real-time. Eventually, multiplexing nanodendrites with targeting biomolecules may provide opportunities for detecting tumors *via* active targeting, real-time *in vivo* visualization of the location within the body, and the potential modulation of their immunostimulating properties in cancer therapy. We strongly believe that the fascinating properties of metallic nanodendrites would attract extensive research in nanomedicine and should open opportunities in the next few decades.

## Conflicts of interest

There are no conflicts to declare.

## Acknowledgements

The authors would like to thank the Institute for Nanotechnology and Water Sustainability (iNanoWS), for financial assistance. The table of contents and Scheme 1 were created using <https://Biorender.com/>.

## References

- 1 A. O. Oladipo, O. S. Oluwafemi, S. P. Songca, A. Sukhbaatar, S. Mori, J. Okajima, A. Komiya, S. Maruyama and T. Kodama, *Sci. Rep.*, 2017, **7**, 45459.
- 2 B. Yameen, W. Il Choi, C. Vilos, A. Swami, J. Shi and O. C. Farokhzad, *J. Controlled Release*, 2014, **190**, 485–499.
- 3 A. M. Bannunah, D. Vllasaliu, J. Lord and S. Stolnik, *Mol. Pharmaceutics*, 2014, **11**, 4363–4373.
- 4 T. Wang, J. Bai, X. Jiang and G. U. Nienhaus, *ACS Nano*, 2012, **6**, 1251–1259.
- 5 A. Dadwal, A. Baldi and R. Kumar Narang, *Artif. Cells, Nanomed., Biotechnol.*, 2018, **46**, 295–305.
- 6 Y. Xin, M. Yin, L. Zhao, F. Meng and L. Luo, *Cancer Biol. Med.*, 2017, **14**, 228–241.
- 7 Y. Dang and J. Guan, *Smart Mater. Med.*, 2020, **1**, 10–19.
- 8 K. Park, *ACS Nano*, 2013, **7**, 7442–7447.
- 9 J. K. Kang, J. C. Kim, Y. Shin, S. M. Han, W. R. Won, J. Her, J. Y. Park and K. T. Oh, *Arch. Pharmacol. Res.*, 2020, **43**, 46–57.
- 10 Y. Liu, K. Deng, J. Yang, X. Wu, X. Fan, M. Tang and Z. Quan, *Chem. Sci.*, 2020, **11**, 4065–4073.
- 11 P. N. Navya and H. K. Daima, *Nano Convergence*, 2016, **3**, 1–14.
- 12 H. T. Nasrabadi, E. Abbasi, S. Davaran, M. Kouhi and A. Akbarzadeh, *Artif. Cells, Nanomed., Biotechnol.*, 2016, **44**, 376–380.
- 13 H. Y. Son, K. R. Kim, C. A. Hong and Y. S. Nam, *ACS Omega*, 2018, **3**, 6683–6691.
- 14 J. J. Lv, A. J. Wang, X. Ma, R. Y. Xiang, J. R. Chen and J. J. Feng, *J. Mater. Chem. A*, 2015, **3**, 290–296.
- 15 A. O. Oladipo, T. T. I. Nkambule, B. B. Mamba and T. A. M. Msagati, *Mater. Sci. Eng., C*, 2020, **110**, 110696.
- 16 W. Li, Z. Sun, D. Tian, I. P. Nevirkovets and S. X. Dou, *J. Appl. Phys.*, 2014, **116**, 033911.
- 17 B. Gómez-Monedero, M. I. González-Sánchez, J. Iniesta, J. Agrisuelas and E. Valero, *Sensors*, 2019, **19**, 1–15.
- 18 W. He, X. Han, H. Jia, J. Cai, Y. Zhou and Z. Zheng, *Sci. Rep.*, 2017, **7**, 1–10.
- 19 I. Robinson, L. D. Tung, S. Maenosono, C. Wälti and N. T. K. Thanh, *Nanoscale*, 2010, **2**, 2624–2630.
- 20 M. Cargnello, R. Agarwal, D. R. Klein, B. T. Diroll, R. Agarwal and C. B. Murray, *Chem. Mater.*, 2015, **27**, 5833–5838.
- 21 Y. Yang, Y. Cao, L. Yang, Z. Huang and N. Long, *Nanomaterials*, 2018, **8**, 208.
- 22 C. Tan, Y. Sun, J. Zheng, D. Wang, Z. Li, H. Zeng, J. Guo, L. Jing and L. Jiang, *Sci. Rep.*, 2017, **7**, 1–10.
- 23 M. Zhang, Y. Zhao, L. Yan, R. Peltier, W. Hui, X. Yao, Y. Cui, X. Chen, H. Sun and Z. Wang, *ACS Appl. Mater. Interfaces*, 2016, **8**, 8834–8840.
- 24 M. Breisch, V. Grasmik, K. Loza, K. Pappert, A. Rostek, N. Ziegler, A. Ludwig, M. Heggen, M. Eppe, J. C. Tiller, T. A. Schildhauer, M. Köller and C. Sengstock, *Nanotechnology*, 2019, **30**, 1–10.
- 25 V. Maney and M. Singh, *Nanomedicine*, 2017, **12**, 1–16.
- 26 J. Stergar, I. Ban, L. Gradišnik and U. Maver, *J. Sol-Gel Sci. Technol.*, 2017, **88**, 57–65.
- 27 P. N. Navya, H. Madhyastha, R. Madhyastha, Y. Nakajima, M. Maruyama, S. P. Srinivas, D. Jain, M. H. Amin, S. K. Bhargava and H. K. Daima, *Mater. Sci. Eng., C*, 2019, **96**, 286–294.
- 28 K. McNamara and S. A. M. Tofail, *Phys. Chem. Chem. Phys.*, 2015, **17**, 27981–27995.
- 29 E. E. Elemike, D. C. Onwudiwe, N. Nundkumar, M. Singh and O. Iyekowa, *Mater. Lett.*, 2019, **243**, 148–152.
- 30 S. Alayoglu, P. Zavalij, B. Eichhorn, Q. Wang, A. I. Frenkel and P. Chupas, *ACS Nano*, 2009, **3**, 3127–3137.



- 31 A. Zaleska-Medynska, M. Marchelek, M. Diak and E. Grabowska, *Adv. Colloid Interface Sci.*, 2016, **229**, 80–107.
- 32 A. C. Anselmo and S. Mitragotri, *Bioeng. Transl. Med.*, 2019, **4**, 1–16.
- 33 Y. Dang and J. Guan, *Smart Mater. Med.*, 2020, **1**, 10–19.
- 34 S. Guo, J. Li, S. Dong and E. Wang, *J. Phys. Chem. C*, 2010, **114**, 15337–15342.
- 35 Y. Feng, X. Ma, L. Han, Z. Peng and J. Yang, *Nanoscale*, 2014, **6**, 6173–6179.
- 36 L. M. Lacroix, C. Gatel, R. Arenal, C. Garcia, S. Lachaize, T. Blon, B. Warot-Fonrose, E. Snoeck, B. Chaudret and G. Viau, *Angew. Chem., Int. Ed.*, 2012, **51**, 4690–4694.
- 37 S. Lu, K. Eid, W. Li, X. Cao, Y. Pan, J. Guo, L. Wang, H. Wang and H. Gu, *Sci. Rep.*, 2016, **6**, 1–11.
- 38 X. Huang, Y. Li, Y. Chen, E. Zhou, Y. Xu, H. Zhou, X. Duan and Y. Huang, *Angew. Chem., Int. Ed.*, 2013, **52**, 2520–2524.
- 39 Y. Zhou, D. Wang and Y. Li, *Chem. Commun.*, 2014, **50**, 6141–6144.
- 40 P. Qiu, M. Yang, X. Qu, Y. Huai, Y. Zhu and C. Mao, *Biomaterials*, 2016, **104**, 138–144.
- 41 A. Fernández-Lodeiro, J. Djafari, D. Lopez-Tejedor, C. Perez-Rizquez, B. Rodríguez-González, J. L. Capelo, J. M. Palomo, C. Lodeiro and J. Fernández-Lodeiro, *Nano Res.*, 2019, **12**, 1083–1092.
- 42 X. Wen, S. Lerch, Z. Wang, B. Aboudiab, A. R. Tehrani-Bagha, E. Olsson and K. Moth-Poulsen, *Langmuir*, 2020, **36**, 1745–1753.
- 43 W. Jia, J. Li and L. Jiang, *ACS Appl. Mater. Interfaces*, 2013, **5**, 6886–6892.
- 44 M. S. S. Bharati, C. Byram and V. R. Soma, *Front. Phys.*, 2018, **6**, 1–13.
- 45 M. Kim, S. Osone, T. Kim, H. Higashi and T. Seto, *KONA Powder Part. J.*, 2017, 80–90.
- 46 L. Xu, S. Li, H. Zhang and D. Wang, *Opt. Express*, 2017, **25**, 3929–3933.
- 47 G. Sharma, A. Kumar, S. Sharma, M. Naushad, R. Prakash Dwivedi, Z. A. AlOthman and G. T. Mola, *J. King Saud Univ., Sci.*, 2019, **31**, 257–269.
- 48 P. Munnik, P. E. De Jongh and K. P. De Jong, *Chem. Rev.*, 2015, **115**, 6687–6718.
- 49 H. Ataee-Esfahani, L. Wang, Y. Nemoto and Y. Yamauchi, *Chem. Mater.*, 2010, **22**, 6310–6318.
- 50 J. Xiong, Y. Wang, Q. Xue and X. Wu, *Green Chem.*, 2011, **13**, 900–904.
- 51 W. Zhang and X. Lu, *Nanotechnol. Rev.*, 2013, **2**, 487–514.
- 52 Y. Li, W. Ding, M. Li, H. Xia, D. Wang and X. Tao, *J. Mater. Chem. A*, 2015, **3**, 368–376.
- 53 Q. Wang, Y. Li, B. Liu, G. Xu, G. Zhang, Q. Zhao and J. Zhang, *J. Power Sources*, 2015, **297**, 59–67.
- 54 H. Wu, S. Mei, X. Cao, J. Zheng, M. Lin, J. Tang, F. Ren, Y. Du, Y. Pan and H. Gu, *Nanotechnology*, 2014, **25**, 195702.
- 55 B. Lim, M. Jiang, P. H. C. Camargo, E. C. Cho, J. Tao, X. Lu, Y. Zhu and Y. Xia, *Science*, 2009, **324**, 1302–1305.
- 56 L. Graham, G. Collins, J. D. Holmes and R. D. Tilley, *Nanoscale*, 2016, **8**, 2867–2874.
- 57 A. G. M. Da Silva, T. S. Rodrigues, S. J. Haigh and P. H. C. Camargo, *Chem. Commun.*, 2017, **53**, 7135–7148.
- 58 H. Wang, Z. Sun, Y. Yang and D. Su, *Nanoscale*, 2013, **5**, 139–142.
- 59 C. Song, Y. Sun, J. Li, C. Dong, J. Zhang, X. Jiang and L. Wang, *Nanoscale*, 2019, **11**, 18881–18893.
- 60 S. Ali, A. S. Sharma, W. Ahmad, M. Zareef, M. M. Hassan, A. Viswadevarayalu, T. Jiao, H. Li and Q. Chen, *Crit. Rev. Anal. Chem.*, 2020, DOI: 10.1080/10408347.2020.1743964.
- 61 K. Shim, W. C. Lee, Y. U. Heo, M. Shahabuddin, M. S. Park, M. S. A. Hossain and J. H. Kim, *Sci. Rep.*, 2019, **9**, 1–7.
- 62 T. Okuno, S. Kato, Y. Hatakeyama, J. Okajima, S. Maruyama, M. Sakamoto, S. Mori and T. Kodama, *J. Controlled Release*, 2013, **172**, 879–884.
- 63 J. L. Li, X. L. Hou, H. C. Bao, L. Sun, B. Tang, J. F. Wang, X. G. Wang and M. Gu, *J. Biomed. Mater. Res., Part A*, 2014, **102**, 2181–2188.
- 64 V. P. Pattani and J. W. Tunnell, *Lasers Surg. Med.*, 2012, **44**, 675–684.
- 65 T. Sugiura, D. Matsuki, J. Okajima, A. Komiya, S. Mori, S. Maruyama and T. Kodama, *Nano Res.*, 2015, **8**, 3842–3852.
- 66 J. Shao, H. Xie, H. Huang, Z. Li, Z. Sun, Y. Xu, Q. Xiao, X. F. Yu, Y. Zhao, H. Zhang, H. Wang and P. K. Chu, *Nat. Commun.*, 2016, **7**, 1–13.
- 67 R. Singh and S. V. Torti, *Adv. Drug Delivery Rev.*, 2013, **65**, 2045–2060.
- 68 K. Zhang, X. Meng, Y. Cao, Z. Yang, H. Dong, Y. Zhang, H. Lu, Z. Shi and X. Zhang, *Adv. Funct. Mater.*, 2018, **28**, 1804634.
- 69 L. Mocan, C. T. Matea, D. Bartos, O. Mosteanu, T. Pop, T. Mocan and C. Iancu, *Clujul Med.*, 2016, **89**, 199–202.
- 70 S. Zhao, X. Zhu, C. Cao, J. Sun and J. Liu, *J. Colloid Interface Sci.*, 2018, **511**, 325–334.
- 71 A. Samadi, H. Klingberg, L. Jauffred, A. Kjær, P. M. Bendix and L. B. Oddershede, *Nanoscale*, 2018, **10**, 9097–9107.
- 72 N. Li, Q. Sun, Z. Yu, X. Gao, W. Pan, X. Wan and B. Tang, *ACS Nano*, 2018, **12**, 5197–5206.
- 73 Z. Wang, Y. Zhang, E. Ju, Z. Liu, F. Cao, Z. Chen, J. Ren and X. Qu, *Nat. Commun.*, 2018, **9**, 3334.
- 74 P. Qiu, M. Yang, X. Qu, Y. Huai, Y. Zhu and C. Mao, *Biomaterials*, 2016, **104**, 138–144.
- 75 D. Matsuki, O. Adewale, S. Horie, J. Okajima, A. Komiya, O. Oluwafemi, S. Maruyama, S. Mori and T. Kodama, *J. Biophotonics*, 2017, **17**, 1–7.
- 76 K. Dong, Z. Liu, Z. Li, J. Ren and X. Qu, *Adv. Mater.*, 2013, **25**, 4452–4458.
- 77 K. Bian, X. Zhang, M. Yang, L. Luo, L. Li, Y. He, C. Cong, X. Li, R. Zhu and D. Gao, *J. Mater. Chem. B*, 2019, **7**, 598–610.
- 78 A. J. McGrath, Y. H. Chien, S. Cheong, D. A. J. Herman, J. Watt, A. M. Henning, L. Gloag, C. S. Yeh and R. D. Tilley, *ACS Nano*, 2015, **9**, 12283–12291.
- 79 Y. Yang, M. Chen, Y. Wu, P. Wang, Y. Zhao, W. Zhu, Z. Song and X. B. Zhang, *RSC Adv.*, 2019, **9**, 28541–28547.
- 80 G. Borrego-Soto, R. Ortiz-López and A. Rojas-Martínez, *Genet. Mol. Biol.*, 2015, **38**, 420–432.
- 81 X. Liu, X. Zhang, M. Zhu, G. Lin, J. Liu, Z. Zhou, X. Tian and Y. Pan, *ACS Appl. Mater. Interfaces*, 2017, **9**, 279–285.
- 82 J. Zhao, P. Liu and H. Yang, *Int. J. Nanomed.*, 2019, **14**, 9483–9496.



- 83 C. Hwang, J. M. Kim and J. Kim, *J. Radiat. Res.*, 2017, **58**, 405–411.
- 84 X. J. Zheng and J. C. L. Chow, *World J. Radiol.*, 2017, **9**, 63.
- 85 M. A. Muhammad, R. A. Rashid, R. M. Lazim, N. Dollah, K. A. Razak and W. N. Rahman, *Radiat. Phys. Chem.*, 2018, **150**, 40–45.
- 86 Y. Deng, X. Tian, S. Lu, M. Xie, H. Hu, R. Zhang, F. Lv, L. Cheng, H. Gu, Y. Zhao and Y. Pan, *ACS Appl. Mater. Interfaces*, 2018, **10**, 31106–31113.
- 87 S. Zhu, Z. Gu and Y. Zhao, *Adv. Ther.*, 2018, **1**, 1800050.
- 88 C. Carvalho, R. Santos, S. Cardoso, S. Correia, P. Oliveira, M. Santos and P. Moreira, *Curr. Med. Chem.*, 2009, **16**, 3267–3285.
- 89 Q. Yang, J. Peng, Y. Xiao, W. Li, L. Tan, X. Xu and Z. Qian, *ACS Appl. Mater. Interfaces*, 2018, **10**, 150–164.
- 90 Y. Liu, X. Zhang, L. Luo, L. Li, R. Y. Zhu, A. Li, Y. He, W. Cao, K. Niu, H. Liu, J. Yang and D. Gao, *Nanomedicine*, 2019, **18**, 303–314.

